frontiers | Frontiers in Robotics and AI

TYPE Original Research
PUBLISHED 13 December 2024
DOI 10.3389/frobt.2024.1431078

OPEN ACCESS

EDITED BY
Jun Ni,
Nanjing Agricultural University, China

REVIEWED BY
Wei Lu,
Nanjing Agricultural University, China
Lale Canan Dülger,
İzmir University of Economics, Türkiye
Jun Wu,
Tsinghua University, China

*CORRESPONDENCE
Jianneng Chen,
jiannengchen@zstu.edu.cn

RECEIVED 11 May 2024
ACCEPTED 14 November 2024
PUBLISHED 13 December 2024

CITATION
Zhang L, Zhou H, Chen J, Tong J, Liu Y and Zhang X (2024) Optimization design and experiment of cam-elliptical gear combined vegetables curved surface labeling mechanism.
Front. Robot. AI 11:1431078.
doi: 10.3389/frobt.2024.1431078

Optimization design and experiment of cam-elliptical gear combined vegetables curved surface labeling mechanism

Lei Zhang[1,2], Heng Zhou[1], Jianneng Chen[1,2]*, Junhua Tong[1,2], Yang Liu[1] and Xiaowei Zhang[1]

[1]School of Mechanical Engineering, Zhejiang Sci-Tech University, Hangzhou, Zhejiang, China, [2]Provincial Key Laboratory of Agricultural Intelligent Sensing and Robotics, Hangzhou, Zhejiang, China

To address the problems of the labeling curved surfaces vegetable with long label, such as the label wrinkled and the easy detachment, a cam-elliptical gear combined labeling mechanism with an improved hypocycloid trajectory is proposed. Provide the process of the mechanism, and establish a kinematic model of the mechanism. In order to improve the motion performances of the cam-elliptical gear combined labeling mechanism and avoid labels damage, the NSGA-II algorithm is used to optimize the parameters of the mechanism, resulting in 80 sets of Pareto solutions. The entropy weight TOPSIS method is applied as a quadratic optimization to select an optimal solution from the 80 sets of Pareto solutions and obtain the optimized parameters of the mechanism. A comparative study is conducted with an elliptical-circular planetary gear mechanism using the hypocycloid trajectory. The results show that the improved mechanism reduces the maximum velocity by 7%, the maximum and minimum accelerations by 2% and 18%. After the quadratic optimization the distance error of the center point of suction cup and the labeling point is reduced from 1.3 mm to 0.12 mm, and the velocity during labeling and taking position is reduced from 0.10770 m s^{-1} to 0.0037 m s^{-1}. The correctness of the proposed method is validated through simulation studies and experiments. This research provides a theoretical basis for the design and optimization of long label and curved surface labeling mechanism for vegetables.

KEYWORDS

improved hypocycloid trajectory, cam-elliptical gear combined mechanism, entropy weight TOPSIS, quadratic optimization, NSGA - II

1 Introduction

Vegetable production is becoming increasingly industrialized (Chen et al., 2023). Unman plant factories are evolving into high-tech facilities characterized by large-scale production and widespread use of technology (Zhang and Kacira, 2022; Jin et al., 2022a; Jin et al., 2022b) Labeling machines play an important role in the packaging of unmanned plant factories. Currently, the widely preferred labeling equipment includes blow-type labeling machines and bottle labeling machines, which can-not meet the long label labeling needs of curved surface vegetables.

Many scholars have conducted research on the labeling machines, such as Zhang et al. (2012) have designed a virtual prototype of a high-speed labeling mechanism based on Eon Studio software, but it has not been tested to verify its reliability. Cho and Bhushan (2016) studied the dam-age to labels caused by different labeling mechanism mate-rials, this provides a reference for the material selection of the labeling mechanism. Salamandra (2017) used light-sensitive sensors to locate the position of labels and improved labeling accuracy. In addition, the application of robots in labeling operations has also received attention (Wu et al., 2009a; Wu et al., 2009b; Wu et al., 2009c).

Sirkett et al. (2006), Sirkett et al. (2007) applied a spur gear planetary gear train with an hypocycloid trajectory to take the box, and verified its feasibility by finite element analysis method, but it did not establish mathematical modeling for a planetary gear train with an hypocycloid trajectory. Tong et al. (2018) designed an elliptical-circular gear planetary gear train mechanism, and established a kinematic model. It took a lot of time to obtain a set of optimal solutions by means of human-computer interaction, and proved the feasibility of the mechanism through comparative study. The lack of experiments verification does not prove whether it is feasible in real production. At the same time, the hypocycloid trajectory has been widely used in the mod-ern machinery industry (Mo et al., 2023; Toshinori and Ryota, 2023).

In terms of multi-objective optimization algorithms, Srinivas and Deb (Srinivas and Deb, 1995) proposed the NSGA. Cho and Lee (2017) focuses on the Multi-objective optimum design of tire structure using genetic algorithm. Xiong et al. (2018) used MOPSO and TOPSIS (Technique for Order Preference by Similarity to Ideal Solution) to optimize the weight of the car body. Leal-Naranjo et al. (2019) conducted a comparative study on the multi-objective optimization methods NGSA-II, MOPSO and MOEA/D, it found that MOEA/D was more suitable for the dimensional synthesis of a spherical parallel manipulator. Palakonda and Kang (2023) proposed a Pre-DEMO on the basis of MODEA, and proved the correctness of the proposed algorithm through comparative study. Comparative study. Zhang et al. (2023) proposed a Grey Relation Analysis method for the secondary optimization of parameters after multi-objective optimization, which provided inspiration for avoiding human factor interference in the selection of optimal parameters in this paper.

In this study, the cam-elliptical gear combined mechanism is used to complete the curved surface labeling of vegetables. The specific research contents are as follows: establish a kinematics model of the cam-elliptic gear combined mechanism with an improved hypocycloidal trajectory, and give the labeling process. The parameters of the mechanism are optimized by multi-objective optimization method NSGA-II and entropy weight TOPSIS method. According to the optimized parameters, a three-dimensional model of the cam-elliptical gear combined mechanism is established. The correctness of the mechanism is verified by theoretical analysis and simulation.

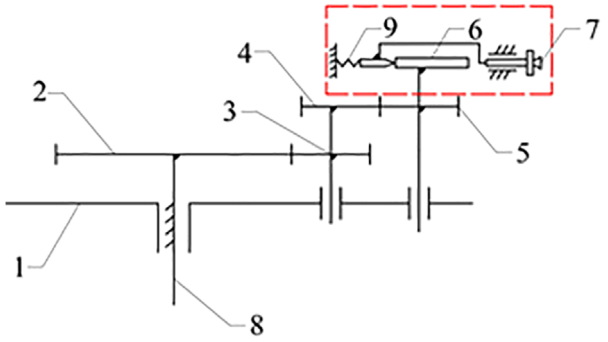

FIGURE 1
Cam-elliptical gear combined labeling mechanism: 1. rotating bracket 2. sun gear 3. spur idler gear 4. elliptical idler gear 5. elliptical planet gear 6. cam 7. labeling actuator 8. fixed shaft 9. spring.

2 Materials and methods

2.1 Principle and process of the mechanism

The cam-elliptical gear combined labeling mechanism is shown in Figure 1. Its working principle is as follows: the rotating bracket one rotates around the fixed shaft 8. The sun gear 2 is fixed to the fixed shaft. The spur idler gear 3 and the elliptical idler gear 4 are fixed on the coaxial, and the elliptical idler gear is engaged with the elliptical planet gear 5. The cam 6 in the red line is coaxial with the elliptical planet gear, and the cam lever is placed behind the cam. The cam lever maintains contact with the cam through the action of spring 9. When the suction cup contacts the surface of the labeling object, the actuator 7 moves backward due to the action of the spring, thus achieving the purpose of flexible labeling.

The process of cam-elliptical gear combined labeling mechanism is shown in Figure 2A. During the labeling process, the moment when the suction cup on the labeling actuator makes contact with the label is considered the starting point of the labeling action. Firstly, the suction cup adsorbs the label, then the planetary gear train drives the actuator to follow the planetary gear rotation. When arriving at the labeling station, the suction cup affixes the label to the labeling object in the order of first right, then middle, and finally left. The operation is summarized in Figure 2B, which shows the different points in its travel.

2.2 The model of cam-elliptical gear combined labeling mechanism

2.2.1 Mathematical model of cam-elliptical gear labeling mechanism

The structure diagram of C&E labeling mechanism is shown in Figure 3. The symbols in the figure are defined as shows in Table 1.

Take O_1 as the origin to establish a rectangular coordinate system as shown in Figure 4. The conditions for forming a hypocycloid trajectory, that is, the trajectory of the point of J, are as follows: the radius ratio of the sun gear, the idler gear and the planetary gear is 3:1:1; The initial angle between O_1O_3 and the x-axis is θ_0 equals $\pi/6$; The elliptical idler gear is the same size as the elliptical

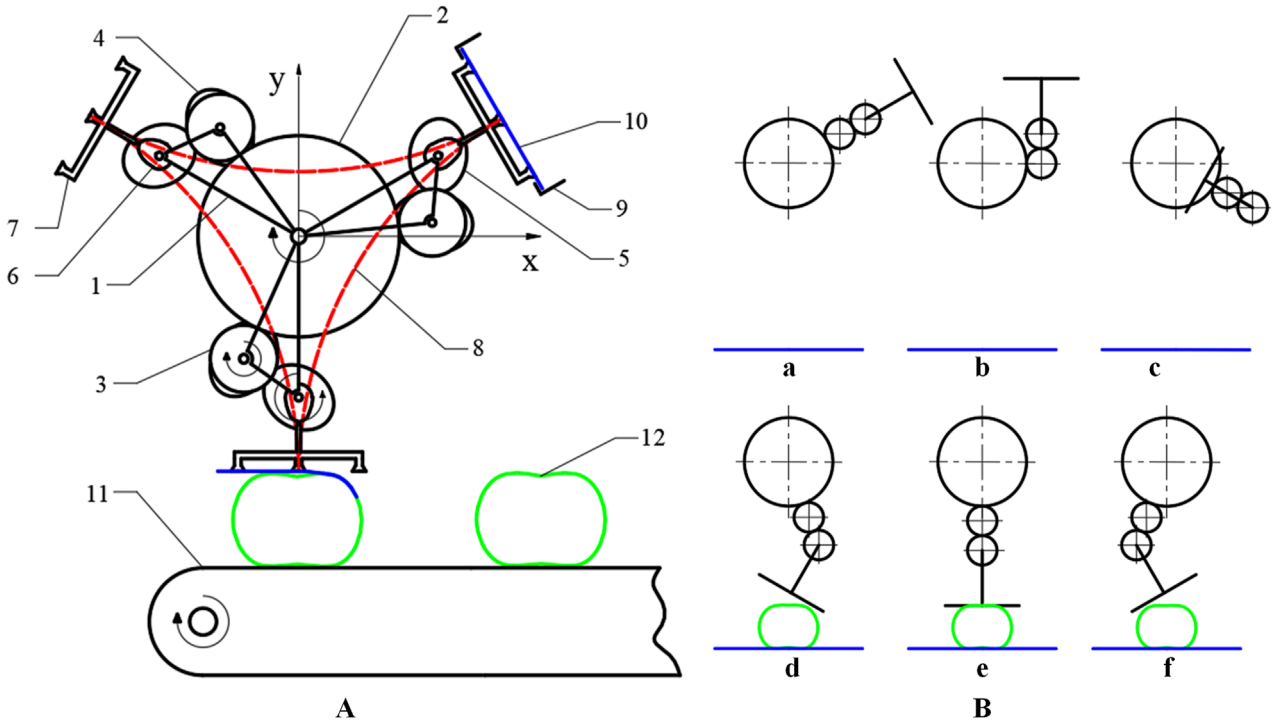

FIGURE 2
The process of cam-elliptical gear combined labeling mechanism **(A)**. 1. rotating bracket 2. sun gear 3. spur idler gear 4. elliptical idler gear 5. elliptical planet gear 6. cam 7. labeling actuator 8. Hypocycloid trajectory 9. label tray 10. label 11. conveyor 12. label object; **(B)** a-f is the different points in its travel.

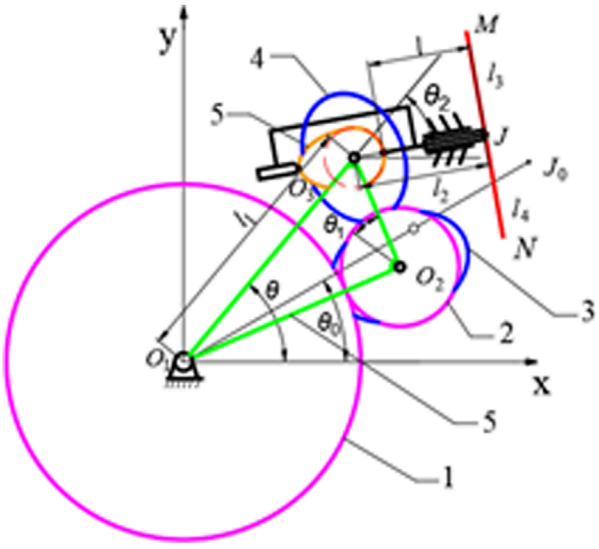

FIGURE 3
Structure diagram of C&E labeling mechanism 1. sun gear 2. circular idler gear 3. elliptical idler gear 4. Elliptical planetary gear 5. Cam 6. Rotating bracket.

planetary gear. Therefore, when the rotating bracket rotates (θ-θ_0), the elliptical planet gear will rotate 3(θ-θ_0), that is, the suction cup will rotate from point J to J_0. Establishes the displacement equation of the center point J of the elliptical-circular gear planetary gear train is in Equation 1:

$$\begin{cases} x = l_1 \cos\theta + l_2 \cos(\theta - \theta_2) \\ y = l_1 \sin\theta + l_2 \sin(\theta - \theta_2) \end{cases} \tag{1}$$

Displacement equation of the center point M of the right suction cup is in Equation 2:

$$\begin{cases} x = l_1 \cos\theta + l_2 \cos(\theta - \theta_2) - l_3 \cos(\theta - \theta_2) \\ y = l_1 \sin\theta + l_2 \sin(\theta - \theta_2) + l_3 \sin(\theta - \theta_2) \end{cases} \tag{2}$$

Displacement equation of the center point N of the left suction cup is in Equation 3:

$$\begin{cases} x = l_1 \cos\theta + l_2 \cos(\theta - \theta_2) + l_4 \cos(\theta - \theta_2) \\ y = l_1 \sin\theta + l_2 \sin(\theta - \theta_2) - l_4 \sin(\theta - \theta_2) \end{cases} \tag{3}$$

where θ_2 is the rotation angle of the elliptical planetary gear relative to O_2O_3; l_4 is the distance between the point J and point N; α is the independent variable of the angle of the elliptical idler gear in Equation 4:

$$\theta_2 = \int_{\sigma_1}^{\sigma_1+\theta_1} i_{21} d\alpha \tag{4}$$

where σ_1 is the angle between the minor axis of the elliptical idler gear and O_2O_3; i_{21} is the transmission ratio of the elliptical gear in Equation 5:

$$i_{21} = \frac{1 - e^2}{1 + 2e\cos\alpha + e^2} \tag{5}$$

TABLE 1 Parameter definition table.

Name	Definition
O_1	Center of the sun gear
O_2	Center of the idler gear
O_3	Center of the elliptical planetary gear
J	Center point of the middle sucker of the labeling actuator
M	Center point of the right sucker of the labeling actuator
N	Center point of the left sucker of the labeling actuator
J_0	Center point of the sucker after the end of the labeling actuator is displaced after O_1O_3 rotation
l	Distance from the intersection of the concentric lines of O_3 and J and the base circle of the cam to J
l_1	Distance between the solar gear center O_1 and the planetary gear center O_3
l_2	Distance between the planetary gear center O_3 and point J
l_3	Distance between the center point J of the middle sucker and the center point M
l_4	Distance between the center point J of the middle sucker and the center point N
θ_0	Initial angle between O_1O_3 and the x-axis
θ_1	The angle of the idler gear
θ_2	The angle of the elliptical planetary gear
σ_1	The angle between the short half axis of the elliptical idler gear and O_2O_3

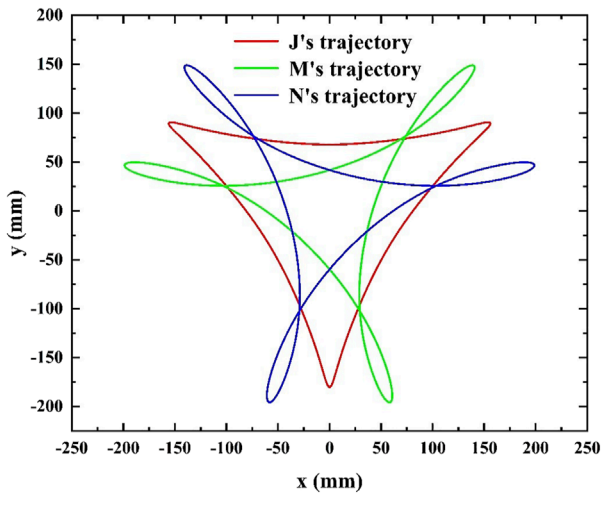

FIGURE 4
Hypocycloid trajectory.

where e is the eccentricity of the elliptical gear.

The trajectory equation of the point J of the cam-elliptical gear combined mechanism is in Equation 6:

$$\begin{cases} x = l_1 \cos\theta + (l+s)\cos(\theta-\theta_2) \\ y = l_1 \sin\theta + (l+s)\sin(\theta-\theta_2) \end{cases} \tag{6}$$

The distance l_2 between the center of the planetary gear and the center point J, which is equal to l plus s, changes with the displacement of the cam push rod, and the change range is $[l_{2\min}, l_{2\max}]$. Where $l_{2\min}$ represents the distance between the cam center and the point J when the cam push rod is about to be pushed travel. $L_{2\max}$ represents the distance when the cam push rod is about to make a return travel.

Where s is the travel of the cam push rod. This paper studies the trajectory of sine acceleration curve cam, and the motion equations are in Equation 7 (Podgornyj et al., 2019):

$$s = \begin{cases} h[1-\cos(\pi\delta/\delta_0)]/2 & ,0 \le \delta < \pi \\ h[1-\cos(\pi\delta/\delta_0)]/2 & ,\pi \le \delta \le 2\pi \end{cases} \tag{7}$$

where s is sine acceleration and constant velocity; δ is the cam motion angle, δ is equal to θ_2; δ_0 is the cam motion angle, $0 \le \delta_0 \le 180°$ is the return travel, $180° \le \delta_0 \le 360°$ is the push travel; h is the stroke of the push rod.

2.2.2 Kinematics model of cam-elliptical gear combined labeling mechanism

The motion performances of the labeled mechanism are related to the rotation angle of the rotating bracket. The rotation velocity is set at 60 rad min^{-1} and the theoretical production efficiency is 180 pcs min^{-1}. The rotation angle of the rotating bracket is θ equals $2\pi t$, and the velocity equation of the point J is in Equation 8:

$$\begin{cases} v_x = -2\pi l_1 \sin 2\pi t - (l+s)\sin(2\pi t-\theta_2)\left(2\pi+\dot{\theta}_2\right) + \dot{s}\cos(2\pi t-\theta_2) \\ v_y = 2\pi l_1 \cos 2\pi t + (l+s)\cos(2\pi t-\theta_2)\left(2\pi+\dot{\theta}_2\right) + \dot{s}\sin(2\pi t-\theta_2) \end{cases} \tag{8}$$

where $\dot{s}$ is the derivative of s; θ_2 is the rotation angle of the elliptical planetary gear relative to O_2O_3 in Equation 9; $\dot{\theta}_2$ is the angular velocity of the elliptical planetary gear is in Equation 10:

$$\theta_2 = \int_0^{2\pi t-\frac{\pi}{2}} \frac{-(e^2-1)}{e^2+2e\cos\alpha+1} d\alpha \tag{9}$$

$$\dot{\theta_2} = \frac{2\pi(e^2-1)}{e^2+2e\cos\left(2\pi t-\frac{\pi}{2}\right)+1} \tag{10}$$

Velocity is in Equation 11:

$$v = \sqrt{{v_x}^2+{v_y}^2} \tag{11}$$

2.3 Parameters optimization based on NSGA-II and entropy weight TOPSIS

An optimization method of cam-elliptical gear labeling mechanism based on NSGA-II and entropy weight TOPSIS is proposed. The Pareto Frontier solution set is obtained by NSGA-II after the first optimization (Kumar et al., 2009; Choi et al., 2021),

and then the entropy weight TOPSIS method is used as a quadratic optimization to obtain the optimal solution of the mechanism parameters. The specific steps of the algorithm are as follows.

① Establishment of objective function:

Set the label starting point X_r: (55, −195), the middle point X_m: (0, −180), the label ending point X_l: (−55, −195), and the arc length from the starting point to the ending point is 135 mm. To ensure that the label on the point M can be successfully attached to the labeling starting point X_r, the distance between the farthest point of the trajectory of the point M and the labeling starting point is optimized as one of the objective functions. This objective function can be expressed in Equation 12:

$$f_1(x) = \min\left(\sqrt{(x_{\max} - x_r)^2 + (y_{\max} - y_r)^2}\right) \tag{12}$$

where $x_{\max}$, $y_{\max}$ are the values of coordinate x and y when the value of f_0 (x,y) is the largest, which can be expressed in Equation 13:

$$\max f_0(x,y) = \sqrt{x_{\max}^2 + y_{\max}^2}, x > 0, y < 0 \tag{13}$$

The starting point and ending point of labeling are symmetric about the y-axis. The left and right sides labeling trajectories are also symmetric about the y-axis. Thus, the right side labeling can complete the labeling action, and the left side can also complete the labeling action. Therefore, in the process of optimization, only the distance between the point M and the labeling starting point X_r is taken as the objective function.

Because there is a short touch between the label and the label's plate when taking the label, the label is easy to fall. If the velocity is too fast, the label will be damaged. Therefore, the velocity of the taking station and the labeling station is as small as possible, so the minimum value of the velocity is used as another optimization objective in Equation 14:

$$f_2(x) = \min(v_{\min}) \tag{14}$$

where $v_{\min}$ is the minimum value of the velocity, that is, the value of the velocity when the angle is 0, $2\pi/3$, $4\pi/3$.

Then the optimization model can be expressed in Equation 15:

$$\min F(X) = [f_1(x), f_2(x)]^T \tag{15}$$

② Establishment of target variables in Equation 16:

$$x = [l_1 \ \ l_2 c a l_3] \tag{16}$$

③ Establishment of constraint conditions:

To ensure smooth operation of the elliptical gear without pulsation (Bair, 2004) $[(a+c)/(a-c)]^2 \le 5$; To ensure that the mechanism can complete the hypocycloidal trajectory, the relationship between l_1 and $l_{2\max}$ is $-l_1+2l_{2\max} \le -1$; To ensure that the middle suction cup can reach the labeling point, $l_1 + (l_{2\max} + s) = 180$; In order to get the proper distance between the middle sucker and the right sucker, $-l_{2\max} + l_3 \le 20$. The constraint equation can be established in Equation 17:

$$s.t. \begin{cases} \left(\frac{a+c}{a-c}\right)^2 \le 5 \\ -l_1 + 2l_2 \le 1 \\ l_1 + l_2 = 172 \\ -l_2 + l_3 \le 20 \end{cases} \tag{17}$$

According to the parameters of the labeled object, the value range of each variable is considered comprehensively in Equation 18:

$$s.t. \begin{cases} 100 \le l_1 \le 140 \\ 50 \le l_2 \le 70 \\ 1 \le c \le 20 \\ 20 \le a \le 50 \\ 35 \le l_3 \le 85 \end{cases} \tag{18}$$

④ Establishment of the original decision matrix:

The performance index of Pareto Frontier solution obtained by NSGA-II optimization is transformed into the original decision matrix in TOPSIS method in Equation 19:

$$X = \begin{pmatrix} x_{11} & x_{12} & \cdots & x_{1n} \\ x_{21} & x_{22} & \cdots & x_{2n} \\ \vdots & \vdots & \ddots & \vdots \\ x_{m1} & x_{m2} & \cdots & x_{mn} \end{pmatrix} \tag{19}$$

where X is the original decision matrix, x_{ij} represents the j index value of the i scheme, i = 1,2, … m, j = 1,2, … n, x_{ij} in this study is the Pareto solutions obtained by NSGA-II algorithm, m = 80, n = 2.

⑤ Establishment of regular matrix:

In order to eliminate the effects of different dimensions, each element of the original matrix needs to be normalized in Equation 20:

$$z_{ij} = a_{ij} / \sum_{i=1}^{m} a_{ij} \tag{20}$$

The regular matrix can be obtained in Equation 21:

$$Z_{ij} = \begin{pmatrix} z_{11} & z_{12} & \cdots & z_{1n} \\ z_{21} & z_{22} & \cdots & z_{2n} \\ \vdots & \vdots & \cdots & \vdots \\ z_{m1} & z_{m2} & \cdots & z_{mn} \end{pmatrix} \tag{21}$$

⑥ Determine entropy weight and information entropy:

The information entropy and weight coefficient of each performance index of cam-elliptical gear combined labeling machine were calculated, respectively. The calculation formula of information entropy is in Equation 22:

$$H_j = -\frac{1}{\ln(m)} \sum_{i=1}^{m} z_{ij} \ln\left(z_{ij}\right) \tag{22}$$

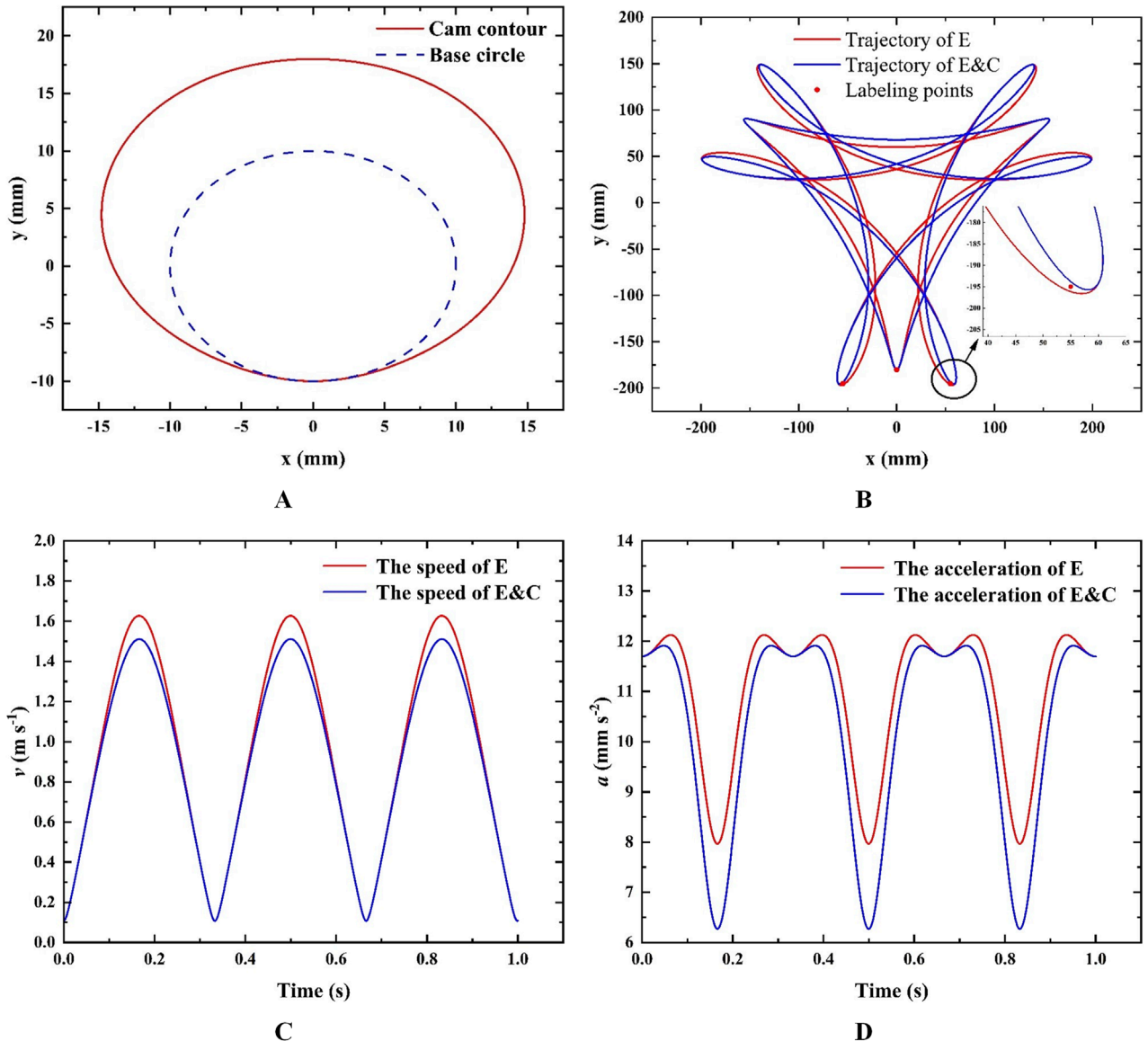

FIGURE 5
(A) Cam profile; **(B)** Track curve; **(C)** Velocity comparison; **(D)** Acceleration comparison.

The calculation formula of entropy weight coefficient is in Equation 23:

$$\omega_j = \left(1 - H_j\right) / \left(m - \sum_{j=1}^{m} H_j\right) \tag{23}$$

⑦ Calculate the normalized score:

Determine positive and negative ideal solutions in Equation 24:

$$\begin{cases} Z^+ = \left(Z_1^+, Z_2^+, \cdots, Z_m^+\right) \\ = \left(\max\left(z_{11}, z_{21}, \cdots, z_{n1}\right), \max\left(z_{12}, z_{22}, \cdots, z_{n2}\right), \cdots, \max\left(z_{1m}, z_{2m}, \cdots, z_{nm}\right)\right) \\ Z^- = \left(Z_1^-, Z_2^-, \cdots, Z_m^-\right) \\ = \left(\min\left(z_{11}, z_{21}, \cdots, z_{n1}\right), \min\left(z_{12}, z_{22}, \cdots, z_{n2}\right), \cdots, \min\left(z_{1m}, z_{2m}, \cdots, z_{nm}\right)\right) \end{cases} \tag{24}$$

where Z^+ and Z^- represent positive ideal solution set and negative ideal solution set, respectively; Z_m^+ represents the largest number in each column and Z_m^- represents the smallest number in each column.

TOPSIS method uses the Euclidean distance between each index and the positive and negative ideal solution to select its advantages and disadvantages.The corresponding calculation formula is in Equation 25:

$$\begin{cases} D_i^+ = \sqrt{\sum_{j=1}^{m} \omega_j \left(Z_{ij} - Z_j^+\right)^2} \\ D_i^- = \sqrt{\sum_{j=1}^{m} \omega_j \left(Z_{ij} - Z_j^-\right)^2} \end{cases} \tag{25}$$

TABLE 2 Comparison of motion performances after adding cam.

	Distance error (mm)	Maximum velocity (m s^{-1})	Maximum acceleration (mm s^{-2})	Minimum acceleration (mm s^{-2})
E labeling mechanism	2.3	1.668	12,660	8,222
E&C labeling mechanism	1.3	1.552	12,384	7,528
difference Value	1	0.116	276	1,694
Percentage	43%	7%	2%	18%

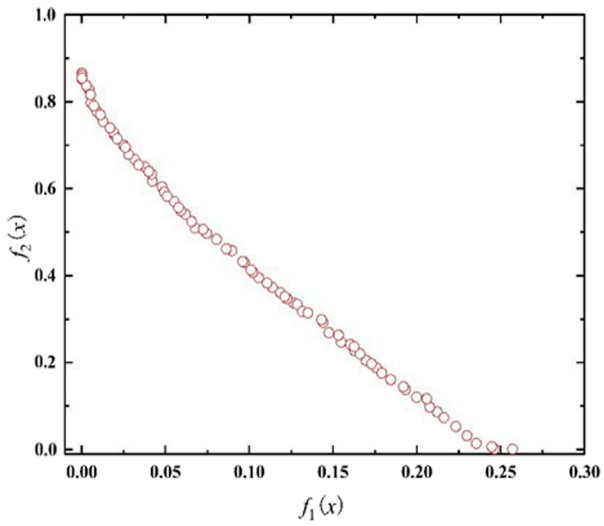

FIGURE 6
Pareto sets.

TABLE 3 Information entropy and entropy weight of each evaluation index.

Evaluation index	Information entropy	Entropy weight
$f_1(x)$	0.968	39.247
$f_2(x)$	0.951	60.753

TABLE 4 The relative closeness between each scheme and the ideal solution.

Ranking	D_i^+	D_i^-	S	Projects
1	0.464	0.650	0.584	67
2	0.472	0.660	0.583	40
⋮				
79	0.775	0.626	0.447	2
80	0.779	0.626	0.445	1

Calculate the normalized score in Equation 26:

$$S = \frac{D_i^-}{D_i^+ + D_i^-} \tag{26}$$

where $0 \le S \le 1$, the closer the value of S is to 1, and the larger the value of D_i^+, it indicates that the evaluation effect of the proposed solution is superior (Qu et al., 2023).

3 Results

3.1 Optimization results of cam-elliptical gear combined labeling mechanism

3.1.1 The results of the comparative study

The parameters of the cam-elliptical gear combined labeling mechanism are initially selected: take l_1 as 120, l as 52, l_3 as 60, c as one and a as 20. Take the radius of the base circle of the cam r_0 as 10, take stroke s as 8. By applying the parameters into Equation 7, the contour of the cam can be obtained, resulting in the visualization shown in Figure 5A. Similar comparative analysis is made on the cam-elliptical gear combined labeling mechanism. Perform a comparative analysis of the cam-elliptical gear combined labeling mechanism (For ease of narration, the legend in Figure 5 uses E&C instead of the cam-elliptical gear combined labeling mechanism), and obtain the hypocycloid trajectory, velocity curve, and acceleration curve for the elliptical-circular gear planetary gear labeling mechanism (For ease of narration, the legend in Figure 5 uses E instead of the elliptical-circular gear planetary gear labeling mechanism). Compare it with the cam-elliptical gear combined label applicator mechanism as shown in Figure 5. The distance error of the point M and the point X_r, as well as the maximum velocity, maximum acceleration and minimum acceleration of the point J trajectory are compared, as shown in Table 2. It can be seen that the distance error is reduced from 2.3 mm to 1.3 mm, the maximum velocity is reduced by 7%, and the minimum acceleration is reduced by 18%. Maximum acceleration reduced by 2%.

The results show that the cam-elliptical gear labeling mechanism has better motion performances. Although the motion performances are improved, it can be seen from Figure 5C and Table 2 that there is a certain distance error of the maximum point M trajectory and the point X_r. And there is still a

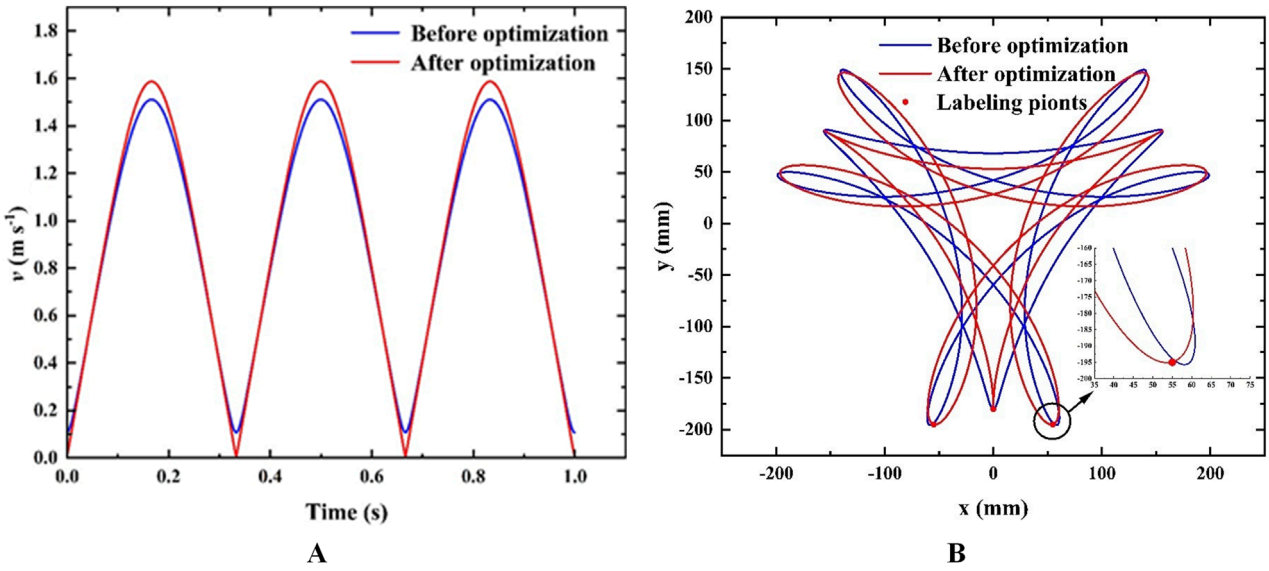

FIGURE 7
(A) Optimized trajectory comparison; **(B)** Optimized velocity comparison.

TABLE 5 Comparison of optimization results.

	Distance error (mm)	Labeling velocity (m s^{-1})
Before optimization	1.30	0.10770
After optimization	0.12	0.0037

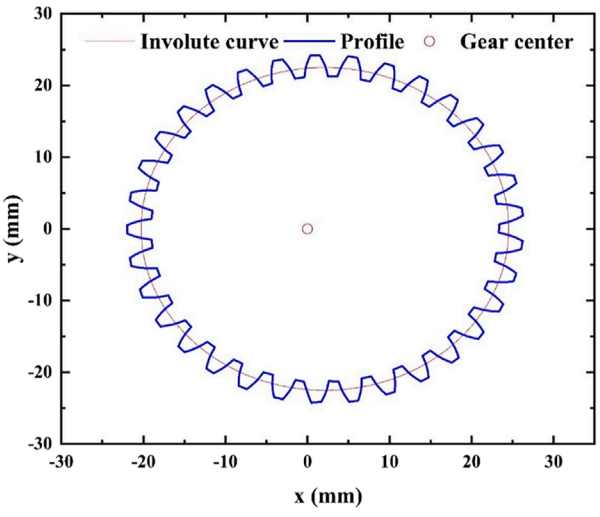

FIGURE 8
Pitch curve and tooth profile of elliptical gear.

certain velocity in the taking and labeling station, which affects the marking and labeling effect. Therefore, it is necessary to optimize the parameters of the mechanism.

3.1.2 Result of the optimization

Set the population number be 200, the maximum genetic algebra be 800, and the crossover probability be 0.4. The optimal Frontier of Pareto is shown in Figure 6. It can be seen that eighty sets of Pareto solutions are smooth as a whole, and the solution sets is evenly distributed, it shows that the optimization results are good. The optimization results indicate that there are mutual constraints between the objectives and the optimal solution cannot be obtained at the same time.

Therefore, the entropy weight TOPSIS method is used as a quadratic optimization to evaluate the 80 of solutions and find an optimal solution. The eighty sets of Pareto solutions obtained from calculations are taken as the candidate decision solutions. The information entropy and entropy weight of the minimum distance $f_1(x)$ and minimum velocity $f_2(x)$ are calculated and shown in Table 3. The relative closeness between each scheme and the ideal solution is shown in Table 4. At the end, the 67th set of solutions is selected as the optimal solution with the parameters: take l_1 as 114.23, l as 57.77, c as 1.06, a as 22.75 and l_3 as 60.04. Comparing the trajectory of the point J, the point N, and the point M before and after optimization, and the velocity of J, as shown in Figures 7A, B.

The distance error of the maximum point of the M trajectory and the point X_r before and after optimization, and the velocity of the point J in labeling and taking station, are shown in Table 5.

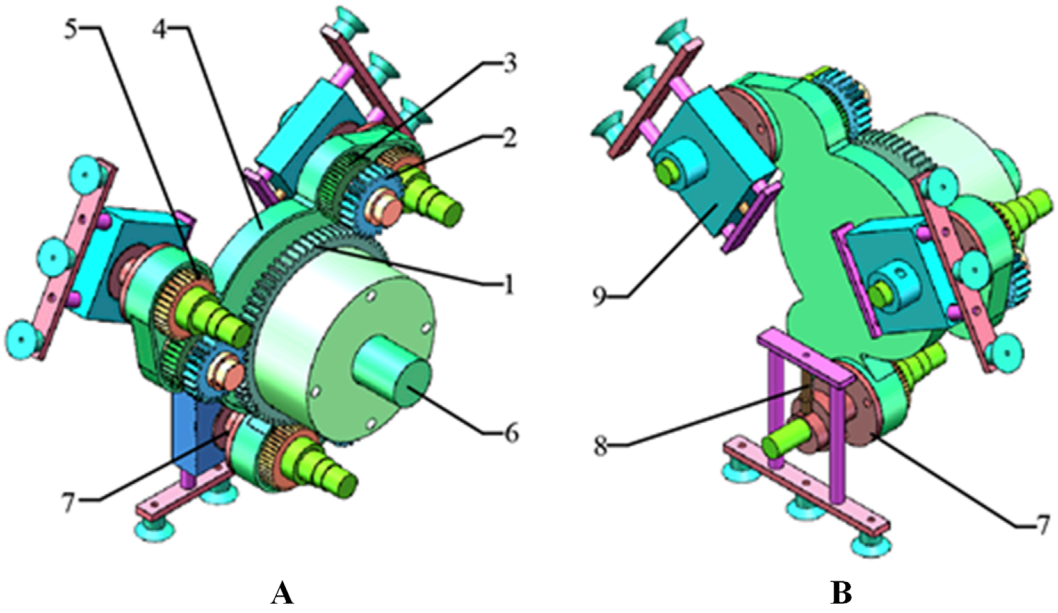

FIGURE 9
Three-dimensional model of cam-elliptical gear combined labeling mechanism: **(A)** The back of mechanism, 1. sun gear 2. idler gear 3. elliptical idler gear 4. rotating bracket 5. elliptical planetary gear 6. fixed shaft 7. cam; **(B)** The front of mechanism, 8. cam lever, 9. sliding sleeve.

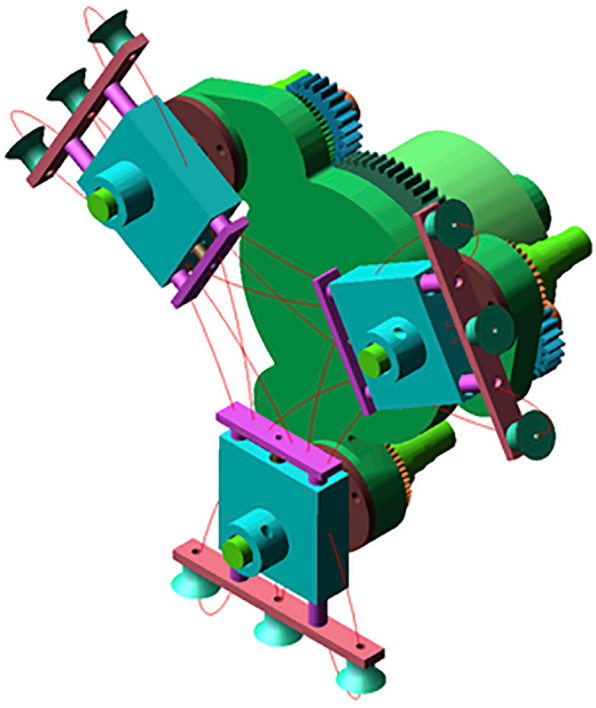

FIGURE 10
Simulation trajectory.

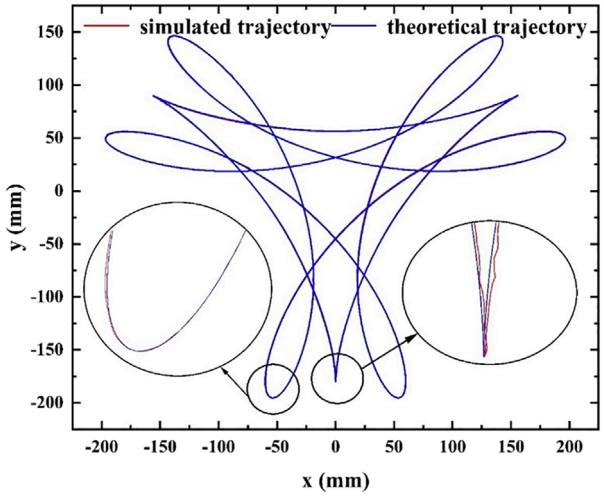

FIGURE 11
Comparison between simulation trajectory and theoretical trajectory.

The results show that the cam-elliptical gear combined labeling mechanism has better motion performances while achieving the labeling point.

3.2 Results of the simulation and analysis

Based on the optimized parameters, the tooth profile and pitch curve of the elliptical gear are obtained (Bair, 2002; Ye et al., 2019; Marafona et al., 2024), as shown in Figure 8. Established the three-dimensional model of cam-elliptical gear combined labeling mechanism as shown in Figure 9. It can see that the main body of the mechanism is composed of elliptical and circular gear planetary gear train, in a 120° symmetrical arrangement, where the idler gear and planetary gear are installed on the rotating bracket, the labeling

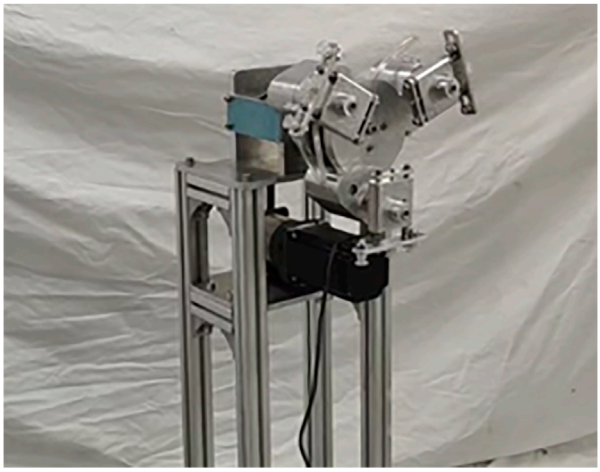

FIGURE 12
Cam-elliptical gear combination vegetables curved surface labeling mechanism.

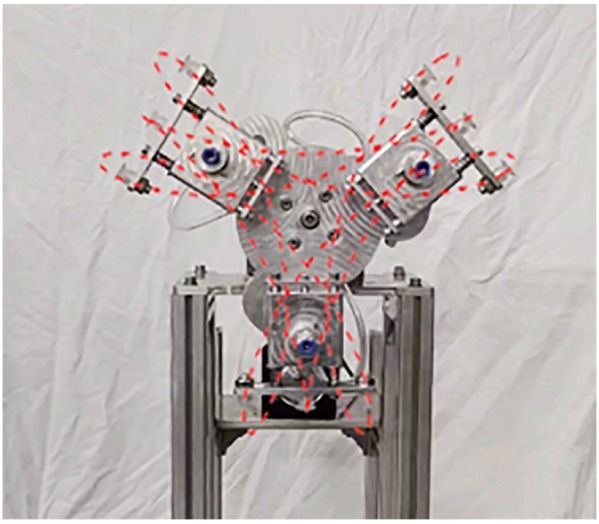

FIGURE 13
Actual trajectory.

actuator is fixed on the planetary gear shaft, and the suction cup is installed on the left end, middle end and right end of the labeling actuator. When the rotating bracket is rotated, the idler gear is driven to rotate around the sun gear, and the idler gear transmits the power to the planetary gear, and the planetary gear drives the labeling actuator to rotate.

To conduct simulation analysis and obtain the simulation trajectory of the cam-elliptical gear combined labeling mechanism, Adams software is utilized. The results of the simulation are depicted in Figure 10. By comparing the theoretical trajectory and the simulation trajectory in Figure 11, it can be seen that the theoretical trajectory and the simulation trajectory are basically the same. The simulation trajectory will fluctuate during the taking and labeling stations, because the gear will collide during operation and cause the fluctuation phenomenon.

3.3 Experiment of cam-elliptical gear labeling mechanism

3.3.1 Construction of cam-elliptical gear combined labeling machine

The two-dimensional drawings of each part of the designed packaging labeling machine are exported by SolidWorks software, and processed according to the drawn two-dimensional drawings. The structure of the whole machine after assembly is shown in Figure 12.

3.3.2 The track verification

Firstly, the test device of the labeling machine is placed in an indoor environment with sufficient light, and the prototype is controlled by the motor controller to achieve the appropriate speed, and the running labeling machine is photographed by the photographic equipment. Then, the video of a running cycle is imported into Adobe Premiere Pro video analysis software, and the running trajectory of J point from mark-taking to labeling to mark-taking process is analyzed frame by frame. Finally, the overall motion trajectory of the point J of the cam-elliptic gear wrapper surface labeling mechanism is obtained, as shown in Figure 13.

Comparing the test trajectory with the theoretical trajectory calculated in Chapter 2.2 with the simulation trajectory obtained by Adams software in Chapter 3.2, the following results are obtained.

(1) Comparing the actual trajectory with the other two trajectories, it can be seen that there is a certain error between the actual trajectory and the other two trajectories in the middle arc segment, but the overall shape and height are not much different. It can be seen from the figure that there is a certain fluctuation in the actual trajectory during the marking and labeling sections. The reason for the fluctuation is that the machining accuracy of the elliptical gear is not enough, and the gap between the teeth does not meet the requirements. In addition, the machining error of other parts, the vibration generated during the installation and operation of the equipment are also the causes of the trajectory formation error.
(2) From the point of view of the running speed of the actual trajectory, the rotation of the cam-elliptic gear packaging dish surface labeling machine prototype. The rotation speed can reach 20 min/rad, and the running speed can reach 60pcs/min due to three sets of labeling actuators.

In summary, the actual trajectory of the cam-elliptical gear packaging dish surface labeling mechanism meets the requirements.

4 Conclusion

(1) To address the curved surface labeling problem of packaged vegetables in unmanned plant factories, the tricuspid hypocycloid was identified as the labeling trajectory, and an improved tricuspid hypocycloid trajectory was proposed, and

the improved tricuspid hypocycloid parametric equation was established.

(2) The mathematical models of cam-elliptical gear combined mechanism and elliptical-circular gear mechanism are established, respectively. The results show that the motion performances of the cam-elliptical gear combined mechanism are improved during the labeling process. Taking the main rotational velocity of 60 rad min^{-1} as an example, the maximum velocity of the point M of the cam-elliptical gear combined mechanism during the labeling process is reduced by 7%, and the maximum and minimum acceleration are reduced by 2% and 18%. The data show that the cam-elliptical gear combined mechanism has better motion performances.

(3) Firstly, NSGA algorithm is used to optimize the cam-elliptical gear combined mechanism, and 80 sets of Pareto solutions are obtained. Then entropy weight TOPSIS method is used as a quadratic optimization to select a set of optimal solutions. Secondly, the 67th set of solutions is selected as the optimal solution. The distance error of the maximum point of the point M and the starting point X_r is reduced from 1.30 mm to 0.12 mm, and the velocity at the labeling and taking station is reduced from 0.10770 m s^{-1} to 0.0037 m s^{-1}. Finally, the correctness of the designed mechanism is verified by experiments.

Data availability statement

The original contributions presented in the study are included in the article/supplementary material, further inquiries can be directed to the corresponding author.

Author contributions

LZ: Writing–review and editing, Conceptualization, Funding acquisition, Project administration. HZ: Conceptualization, Methodology, Visualization, Writing–original draft, Data curation. JC: Funding acquisition, Project administration, Writing–review and editing, Conceptualization, Methodology. JT: Methodology, Investigation, Writing–original draft. YL: Investigation, Writing–review and editing. XZ: Data curation, Writing–review and editing.

Funding

The author(s) declare financial support was received for the research, authorship, and/or publication of this article. This work was supported by the National Key Research and Development Project of China (Grant No. 2021YFD2000704).

Acknowledgments

The authors would like to thank Chuanyu Wu for their help in field management.

Conflict of interest

The authors declare that the research was conducted in the absence of any commercial or financial relationships that could be construed as a potential conflict of interest.

Publisher's note

Supplementary material

The Supplementary Material for this article can be found online at: https://www.frontiersin.org/articles/10.3389/frobt.2024.1431078/full#supplementary-material

References

Bair, B. W. (2002). Computerized tooth profile generation of elliptical gears manufactured by shaper cutters. *J. Mater. Process. Technol.* 122 (2-3), 139–147. doi:10.1016/S0924-0136(01)01242-0

Bair, B. W. (2004). Computer aided design of elliptical gears with circular-arc teeth. *Mech. Mach. Theory* 39 (2), 153–168. doi:10.1016/S0094-114X(03)00111-3

Chen, K., Yuan, Y., Zhao, B., Zhou, L., Niu, K., Jin, X., et al. (2023). Digital twins and data-driven in plant factory: an online monitoring method for vibration evaluation and transplanting quality analysis. *Agriculture* 13 (6), 1165. doi:10.3390/agriculture13061165

Cho, D. H., and Bhushan, B. (2016). Friction and wear of various polymer pairs used for label and wiper in labeling machine. *Tribol. Int.* 98, 10–19. doi:10.1016/j.triboint.2016.02.019

Cho, J. R., and Lee, J. H. (2017). Multi-objective optimum design of TBR tire structure for enhancing the durability using genetic algorithm. *J. Mech. Sci. Technol.* 31 (2017), 5961–5969. doi:10.1007/s12206-017-1140-y

Choi, C., Ahn, H., Yu, J., Han, J. S., Kim, S. C., and Park, Y. J. (2021). Optimization of gear macro-geometry for reducing gear whine noise in agricultural tractor transmission. *Comput. Electron. Agric.* 188, 106358. doi:10.1016/j.compag.2021.106358

Jin, X., Tang, L. M., Li, R. S., Ji, J. T., and Liu, J. (2022b). Selective transplantation method of leafy vegetable seedlings based on ResNet 18 network. *Front. Plant Sci.* 13, 893357. doi:10.3389/fpls.2022.893357

Jin, X., Tang, L. M., Li, R. S., Zhao, B., Ji, J. T., and Ma, Y. D. (2022a). Edge recognition and reduced transplantation loss of leafy vegetable seedlings with Intel RealsSense D415 depth camera. *Comput. Electron. Agric.* 198, 107030. doi:10.1016/j.compag.2022.107030

Kumar, G. V. P., Srivastava, B., and Nagesh, D. S. (2009). Modeling and optimization of parameters of flow rate of paddy rice grains through the horizontal rotating cylindrical drum of drum seeder. *Comput. Electron. Agric.* 65 (1), 26–35. doi:10.1016/j.compag.2008.07.006

Leal-Naranjo, J. A., Soria-Alcaraz, J. A., Miguel, C. R., Juan-Carlos, P. R., Andrés, E., and Horacio, R. G. (2019). Comparison of metaheuristic optimization algorithms

for dimensional synthesis of a spherical parallel manipulator. *Mech. Mach. Theory* 140, 586–600. doi:10.1016/j.mechmachtheory.2019.06.023

Marafona, J. D., Carneiro, G. N., Marques, P. M., Martins, R. C., António, C. C., and Seabra, J. H. (2024). Gear design optimization: stiffness versus dynamics. *Mech. Mach. Theory* 191, 105503. doi:10.1016/j.mechmachtheory.2023.105503

Mo, J. Y., Xu, G., Luo, S. M., Fu, S. P., Chang, X. F., and Liao, L. (2023). Geometric design and dynamic characteristics of a novel abnormal cycloidal gear reducer. *Adv. Mech. Eng.* 15 (3), 5165–5179. doi:10.1177/16878132231158895

Palakonda, V., and Kang, J. M. (2023). Pre-DEMO: Preference-inspired differential evolution for multi/many-objective optimization. *IEEE Trans. Syst. Man. Cybern. Syst.* 53, 7618–7630. doi:10.1109/TSMC.2023.3298690

Podgornyj, Y. I., Skeeba, V. Y., Kirillov, A. V., Martyushev, N. V., and Borisov, M. A. (2019). The synthesis of motion laws for cam mechanisms with additional movement of the follower. *IOP Conf. Ser. Earth Environ. Sci.* 378, 012025. doi:10.1088/1755-1315/378/1/012025

Qu, Z. H., Zhang, P., Hu, Y. H., Yang, H. B., Guo, T. F., Zhang, K., et al. (2023). Optimal design of agricultural mobile robot suspension system based on NSGA-III and TOPSIS. *Agriculture* 13, 207. doi:10.3390/agriculture13010207

Salamandra, B. L. (2017). Analysis of label position stabilization methods on automatic packaging machines. *J. Mach. Manuf. Reliab.* 46, 181–186. doi:10.3103/S1052618817020157

Sirkett, D. M., Hicks, B. J., Berry, C., and Medland, A. J. (2006). Simulating the behaviour of folded cartons during complex packing operations. *Proc. Inst. Mech. Eng. C. J. Mech. Eng. Sci.* 220 (12), 1797–1811. doi:10.1243/0954406JMES109

Sirkett, D. M., Hicks, B. J., Berry, C., and Medland, A. J. (2007). Finite element simulation of folding carton erection failure. *Proc. Inst. Mech. Eng. C. J. Mech. Eng. Sci.* 221 (7), 753–767. doi:10.1243/0954406JMES502

Srinivas, N., and Deb, K. (1995). Muiltiobjective optimization using nondominated sorting in genetic algorithms. *IEEE Trans. Evol. Comput.* 2 (3), 221–248. doi:10.1162/evco.1994.2.3.221

Tong, J. H., Tang, Q. Q., Wu, C. Y., and Luo, H. (2018). Elliptical-circular planetary gear train box-taking mechanism design and trajectory analysis for automatic cartoning machines. *J. Mech. Eng.* 54 (11), 172. (In Chinese). doi:10.3901/JME.2018.11.172

Toshinori, F., and Ryota, T. (2023). Multi-cylinder wind-powered air compressor using hypocycloid motion. *Int. J. Fluid Power Syst.* 16 (1), 17–23. doi:10.5739/jfpsij.16.17

Wu, J., Wang, J., Wang, L., and Li, T. (2009c). Dynamic formulation of redundant and nonredundant parallel manipulators for dynamic parameter identification. *Mechatronics* 19 (4), 586–590. doi:10.1016/j.mechatronics.2009.01.003

Wu, J., Wang, J., Wang, L., Li, T., and Liu, X. (2009b). Workspace and singularity analysis of a 3-DOF planar parallel manipulator with actuation redundancy. *Robotica* 27 (1), 51–57. doi:10.1017/S0263574708004517

Wu, J., Wang, J., Wang, L., Li, T., and You, Z. (2009a). Study on the stiffness of a 5-DOF hybrid machine tool with actuation redundancy. *Mech. Mach. Theory* 44 (2), 289–305. doi:10.1016/j.mechmachtheory.2008.10.001

Xiong, F., Wang, D. F., Ma, Z. D., Chen, S. M., Lv, T. T., and Lu, F. (2018). Structure-material integrated multi-objective lightweight design of the front end structure of automobile body. *Struct. Multidiscipl Optim.* 57, 829–847. doi:10.1007/s00158-017-1778-1

Ye, J., Zhao, X., Wang, Y., Sun, X., Chen, J., and Xia, X. (2019). A novel planar motion generation method based on the synthesis of planetary gear train with noncircular gears. *J. Mech. Sci. Technol.* 33, 4939–4949. doi:10.1007/s12206-019-0933-6

Zhang, L., Liu, Y., Chen, J., Zhou, H., Jiang, Y., Tong, J., et al. (2023). Trajectory synthesis and optimization design of an unmanned five-bar vegetable factory packing machine based on NSGA-II and Grey relation analysis. *Agriculture* 13 (7), 1366. doi:10.3390/agriculture13071366

Zhang, Y., Dou, Y. M., Cai, W. Z., and Zhu, Y. Q. (2012). Virtual manipulation of Eon studio-based for high speed labeling machine. *Appl. Mech. Mater.* 220-223, 57–60. doi:10.4028/www.scientific.net/AMM.220-223.57

Zhang, Y., and Kacira, M. (2022). Analysis of climate uniformity in indoor plant factory system with computational fluid dynamics (CFD). *Biosyst. Eng.* 220, 73–86. doi:10.1016/j.biosystemseng.2022.05.009